Measurements of Thermophysical Properties of Molten Materials from Oscillating and Rotating Drops

Won-Kyu Rhim
Jet Propulsion Laboratory, California Institute of Technology,
4800 Oak Grove Drive, Pasadena, California 91109, USA
and
Takehiko Ishikawa
Space Utilization Research Center, NASDA
Tsukuba, Japan

Abstract

Certain physical properties of a molten drop, levitated, for example, in a high temperature electrostatic levitator can be determined by inducing appropriate mechanical excitations on the drop. Mechanical excitation can be a resonant oscillation or a systematic rotation of a drop. Recent studies have shown that surface tension and viscosity of a low viscosity melt could be determined by inducing a resonant oscillation on the drop, however, these results might be erroneous if the effect of drop rotation that existed during the measurement was not taken into account. If a liquid is a highly viscous, the conventional drop oscillation method no longer applies, requiring a new non-contact method of determining the surface tension and the viscosity. This presentation will begin by showing various mechanical drop excitations that are possible on a levitated molten drop, and application of these excitation methods for the non-contact measurements of electrical resistivity, surface tension and viscosity of melts over a wide viscoisty range will be presented.

1. Introduction

Since Rayleigh's[1] initial calculation of axi-symmetric shapes of rotating drops, the theoretical predictions of drop rotaion processes have been brought to a rare degree of accuracy by Chandrasekhar[2], and more recently by Brown and Scriven[3]. Over the last decade there have been several efforts to experimentally verify these predictions. Rhim, Chung, and Elleman[4] performed an experiment in the ground base using a charged drop levitated by an electrostatic levitator. They rotated the drop exerting acoustic torque, and observed the bifurcation occurring very close to the theoretical prediction. However, the drop which carried electric charges on its surface casted some doubts as a valid system for the verification of the theory which assumed electrically neutral drops. Biswas, Leung, and Trinh[5] studied a rotating drop which was acoustically levitated on the ground base. Using an initially deformed drop (in static state), they obtained results which could expain the results observed during the 1986 Spacelab experiments[6]. Recently Wang, Anilkumar, Lee, and Lin[7] repeated their experiment with improved equipment in the Space Shuttle USML-1. Using spherical drops of silicone oil and glycerin/water mixture, they obtained results that closely agreed with the prediction when the drops rotated satisfying the solid-body-rotation condition. All the above experiments were conducted in ambient conditions where air frictions could have prevented the drops from satisfying a perfect solid-body rotation condition.

This paper describes a new way of conducting drop rotation experiment in a high vacuum using molten metallic drops. In this experiment, the drops rotated in a frictionless environment of vacuum. Therefore, in absence of applied torques, a drop was freely rotating for a long time, eventually reaching a true solid-body rotation state due to the viscosity of the drop. Once the rotation experiment verifies the theory, it can be applied for the measurement of surface tension of the liquid. For low viscosity liquids, the drop oscillation technique[8] is an adequate non-contact technique for the surface tension measurement. However, for high viscosity liquids where drop oscillations cannot be induced, a new non-contact measurement technique for surface tension needs to be developed. For example, viscosities of glass forming

alloy liquids increase nearly 14 orders magnitude as they approach their glass transition temperatures are reached. Finally, we will present an anomalous result observed in a rotating molten tin, which may be explained if the tin isotopes in the drop were separating due to the centrifual force generated by the rotation.

2. Experimental Apparatus and Approach

The basic principle of this experiment was in applying steady (or step-by-step) low-level torque to a molten metallic drop that is being levitated in a high vacuum. The High Temperature Electrostatic Levitator (HTESL) at Jet Propulsion Laboratory levitates a sample about 3 mm in diameter between a pair of parallel disk electrodes that are spaced about 12 mm (Fig. 1). The electric field between these two electrodes produce strong electrostatic force on a charged sample to cancel the downward gravitational force. The four small side electrodes located around the bottom electrode control the sample position along the horizontal directions. The main position control voltage is connected to the upper electrode, while the bottom electrode is electrically grounded through an ac voltage source. This ac voltage source generates oscillating electric field on the drop for the purpose of inducing resonant oscillations. To induce a sample rotation, a four-coil system was mounted on the top electrode. These coils produce a horizontal magnetic field that rotates at an appropriate frequency (400 Hz in the present experiment). The electrode assembly was housed by a stainless steel chamber which was typically evacuated to ~10^{-8} torr. Samples were heated using an xenon arc lamp. A detailed description of the HTESL was given in an earlier publication[9].

Experiments were conducted using a high purity aluminum and a tin samples at approximately 25 K above the respective melting points. Initially, the resonance oscillation of n=2 mode was measured on a non-rotating drop by applying a low-level ac field. Subsequently the ac field was turned off, and the sample rotation was initiated by applying a rotating magnetic field at a preset amplitude and frequency.

The basic principle of the present sample rotation mechanism is essentially the same as asynchronous induction motor. The four-coil assembly works as a stator while levitated sample serves as a rotor. According to the principle of the induction motor[10, 11], if an ac voltage E_1 at frequency ω_s is applied to a stator having a resistance R_1 and an inductance L_1, the torque τ experienced by the rotor (having its own resistance R_2 and inductance L_2) rotating at an instantaneous rotation frequency ω is given by

$$\tau = \frac{\omega_s E_1^2}{R_1^2 + \omega_s^2 L_1^2}\left(\frac{sR_2}{R_2^2 + s^2 L_2^2}\right), \tag{1}$$

where

$$s \equiv \frac{\omega_s - \omega}{\omega_s}. \tag{2}$$

Eq. (1) was tested using a levitated aluminum sphere by measuring the torque for given input parameters as a function of sample rotation frequency. Fig. 2 shows that at a fixed stator current the torque is a linear function of s, i.e. to the instantaneous sample rotational frequency. This means that the relationship $R_2^2 >> s^2L^2$ is well satisfied in Eq. (1), transforming Eq. (1) to a simpler form:

$$\tau = \left(\frac{\omega_s E_1^2}{R_1^2 + \omega_s^2 L_1^2}\right)\frac{1}{R_2}\left(1 - \frac{\omega}{\omega_s}\right). \tag{3}$$

Accurate measurements of sample rotation frequency were important for the determination of torque imparted to the sample. In our experiment, a He-Ne laser beam was directed to the sample, and the reflected beam was detected by a silicon photo-detector. The output voltage of the detector was amplified and digitized to get a Fourier power spectrum, using a micro-computer. Such a power spectrum showed peaks at all harmonics of the sample rotation frequency. Such power spectrum only serves as a coarse indicator of the rotation

frequency. More precise detection of sample rotation was done by exploiting the strobing effect created by a TV monitor. Regular monitors have 30-Hz frame rate (or 60-Hz field rate). A CCD camera operated at the shutter speed 0.001 second was mounted on a tele-microscope to produce a magnified sample image on a TV screen. Whenever the sample rotation rate approached one of the harmonic or sub harmonic frequencies of the 60-Hz field rate, a seemingly static image was appeared on the screen. Such a stroboscopic approach assisted by the power spectrum display allowed us a precise determination of sample rotation frequency without ambiguity.

3. Experiment on Solid Body Rotation.

For drop rotation experiments, we chose a high purity aluminum and a tin sample. All parameters relevant to these samples and experimental conditions are as shown in Table I. Each rotation experiment was initiated by applying a rotating magnetic field to the sample and by video-recording the side view of the drop. Drop rotation frequency was also overlaid on the video images.

As the drops started rotating, nearly sperical initial shape progressively turned into oblate spheroidal shape, and this trend continued until they reached a critical point, the bifurcation point, at which the axisymmetric shape became unstable and it turned into a triaxial ellipsoidal shape. As the drop gained angular momentum , the drop rotation frequency started to decrease even though the drop gained more angular momentum as a result of rapidly increasing moment of inertia. This behavior is in accordance with the earlier ground-base experimental results on rotating charged water drops[4] as well as with the experiments on uncharged drops conducted by Wang et al.[7] in a micro-gravity condition.

Fig. 3 shows the evolution of a normalized drop dimension, R_{max}/R_o, versus the normalized rotation frequency, $\omega_{rot}/\omega_{osc}$, where R_{max} and R_o are the maximum radius of the rotating drop and the radius of spherical shape, respectively. The drop rotation frequency ω_{rot} is normalized by its own oscillation frequency ω_{osc} (n = 2 mode) measured at the non-rotating

state. Also plotted in this figure is the theoretical result calculated by Brown and Scriven[3] showing an initially axi-symmetric drop shape branching out to a two-lobed, three-lobed, or four-lobed drop shape at certain critical frequencies. In reality, however, the two-lobe branch was the one to which the shape transformation from axisymmetric shape took place. Transition between these two branches were reversible as long as the applied torque level was kept sufficiently low to ensure solid body rotation. As one can see in the figure, the experimental points of both the aluminum and tin drops follow the theoretical curve within 2%. We observe that the data points along the axi-symmetric branch are slightly below the theoretical curve. This was caused due to the slightly oblate spherical shape of the drop in initially non-rotating state. The observed bifurcation point also agrees with the predicted value, $\omega_{rot}/\omega_{osc} = 0.559$, within 2%. Fig. 4 shows the side views of the rotating aluminum drop corresponding to the data points indicated in Fig. 3. The points **a**, **b**, **c**, and **d** correspond to axi-symmetric shapes. However, at the point **d**, a quick transition took place from an axi-symmetric to a triaxial ellipsoidal shape (to the point **e** on the two-lobed branch). With further gaining of angular momentum, the drop shape changed to **f**. When the angular momentum was reduced by small step by step, the drop followed the two-lobed branch down to the predicted bifurcation point.

An anomalous behavior was observed when a rotating experiment was performed with a molten tin drop (39.8 mg). When the drop was rotated at a high torque level which produced overshooting beyond the predicted bifurcation point (see Fig. 5). The drop angular momentum was further increased to a point where R_{max}/R_o was approximately 1.6. Applied torque was turned off at this point, allowing the drop to rotate freely (in the frictionless vacuum) for the next two hours at the same temperature. Now, when the drop angular momentum was slowly reduced under the influence of negative torque, surprisingly the drop shape evolved following a quite different path away from the theoretical branches. In fact, the drop shape remained as triaxial ellipsoidal all the way down to the non-rotating state, completely by-passing the axi-symmetric branch. When the rotation frequency was slowed down to approximately 10 Hz, the drop (originally with its longest axis perpendicular to the vertical rotation axis) became

unstable, and it eventually aligned its longest axis along the gravity field as the angular momentum was further reduced. The final shape and orientation of the drop is shown in Fig. 6. The cause of this anomaly is not understood at this moment. Present authors only speculate that the probable cause might be isotopes in the rotating tin drop separating under the influence of centrifugal force, although we failed to confirm this using the Secondary Ion Mass Spectrometer. Tin has seven highly abundant isotopes between ^{116}Sn (14.53%) and ^{124}Sn (5.79%), among which ^{120}Sn (32.59%) is the most abundant isotope. An anomaly similar to tin samples could not be observed in molten aluminum. In natural aluminum, ^{27}Al is essentially the only isotope. If we consider a sphere, 1.5 mm in radius, that is rotating at 50-Hz, the difference in centrifugal acceleration between the center and the surface of the drop is as much as 15 times the Earth gravitational acceleration. More systematic experiments and some theoretical modeling are required before understanding of such behavior can be obtained.

4. Application to Surface Tension Measurement

In this section the possibility of measuring surface tension by drop rotating will be investigated. For low viscosity liquids, measurement of a resonant oscillation of levitated drop is an accurate means of extracting its surface tension[8]. However, the accuracy of this method decreases as the damping constant of free oscillation becomes shorter, due to increasing viscosity.

If a drop rotates according to the theoretical curve as shown in Fig.3, one can determine the oscillation frequency, ω_{osc}, at any point of the curve, if the shape parameter, R_{max}/R_o, and the rotation frequency, ω_{rot}, are known. We notice that liquid viscosity does not play any role in the theory of rotating drops as long as the drop can reach the condition of solid-body rotation. Higher viscosity will only help to bring the solid-body condition quickly. A proposal of measuring surface tension using drop rotation was made early on by Elleman et al.[12]. Since the drop rotation frequency of an axi-symmetric drop is difficult to measure if the drop surface is extremely uniform, the drop rotation frequency should be made on the triaxial branch

close to the bifurcation point. Since $\omega_{rot}/\omega_{osc}= 0.559$ at the bifurcation point, and ω_{rot} can be measured, ω_{osc} is determined. This approach for surface tension measurement should be applicable to metallic melts regardless of their viscosity, if the solid-body rotation condition is respected.

In this section, we intend to systematically verify this surface tension measurement approach using a molten tin and an aluminum drop. Since both drops showed surface structure caused by oxide layers, we could also measure the drop rotation frequencies along the axi-symmetric branch, using the rotation detection method described in a previous section. To obtain a more amplified view of drop shape changes, the axi-symmetric values of the two rotating melts and the theoretical points were plotted in Fig.7 in terms of R_{max}/R_{min} instead of $R_{max}/R_{o,}$ where R_{min} is the vertical dimension of the rotating drop. (Aluminum data in Fig. 7 are not the same set of data shown in Fig. 3.) At their static states ($\omega_{rot.} = 0$), both drops showed slight elongation along the vertical direction. We searched for appropriate multiplication factors (one for the aluminum and one for the tin, respectively), which would make $R_{max}/R_{min} = 1$ at $\omega_{rot}/\omega_{osc} = 0$, and apply them to the respective set of data as shown in Fig. 8. As one can see, agreement between these two sets of data is very good. Since aluminum data showed very close agreement with the theory as demonstrated in Fig. 3, let us assume that the best fit curve to axi-symmetric points of aluminum data overlaps the theoretical curve if it is plotted in the R_{max}/R_{min} scale. The fitting curve can be expressed by

$$R_{max}/R_{min} = 1 - 6.655 \times 10^{-2} F + 1.663 F^2 - 2.669 F^3 + 4.445 F^4 \qquad (4)$$

where $F= \omega_{rot}/\omega_{osc}$. For every experimental data in Fig. 8, R_{max}/R_{min} and ω_{rot} are known. Therefore, ω_{osc} can be determined from Eq. (4) for all points on the curve. These are plotted against $\omega_{rot}/\omega_{osc}$ in Fig. 9 and compared with the directly measured oscillation frequency. From the figure one can see the effective oscillation frequencies obtained from the drop of smaller deformation show larger uncertainties, while those which correspond to higher

rotational frequency rapidly converge to the actual oscillation frequency within ±2 % (which corresponds to ±2 Hz for the tin drop). The oscillation frequency directly measured on the molten tin drop are usually reproducible within 0.5 Hz. Also noticeable in Fig. 9 is that the oscillation frequency determined by the overshot points show rather strong divergence from the actual frequency.

Under the assumption of a uniform distribution of surface charge, ω_{osc} so obtained is related to the surface tension of the liquid σ by[13]

$$\omega_{osc.}^2 = \frac{8\sigma}{\rho r_o^3}\left(1 - \frac{Q_s^2}{64\pi^2 r_o^3 \sigma \varepsilon_o}\right), \tag{5}$$

where ρ is the liquid density, r_o is the radius of the static spherical drop, and ε_o is the permitivity of the vacuum. The surface charge Q_s can be determined from the levitation condition between two flat parallel electrodes:

$$mg = \frac{Q_s V}{L}, \tag{6}$$

where m is the sample mass, g is the gravitational acceleration, V is the potential difference between the electrodes, and L is the spacing between electrodes. Strictly speaking, the shape of a drop which is levitated by an electric force against the gravity deviates from a perfect sphere, and the surface charges are not distributed uniformly. Oscillation of an electrostatically levitated drop in such a non-ideal situation has been examined recently by Feng and Beard[14], using the multiple parameter perturbation method. Their frequency correction term for axisymmetric n=2 mode is given by

$$\omega_{2c+}^2 = \omega_{osc.}^2 [1 - F(\sigma, q, e)], \tag{7}$$

where ω_{2c+} is the measured frequency, ω_{osc} is defined by Eq. (5), and q and e are defined by

$$q^2 \equiv \frac{Q_i^2}{16\pi^2 r_o^3 \varepsilon_o}, \tag{8}$$

and

$$e^2 \equiv E^2 r_o \varepsilon_o, \tag{9}$$

respectively, where E is the applied electric field. $F(\sigma, q, e)$ in Eq. (7) is defined by

$$F(\sigma,q,e) \equiv \frac{(243.31\sigma^2 - 63.14q^2\sigma + 1.54q^4)e^2}{176\sigma^3 - 120q^2\sigma^2 + 27\sigma q^4 - 2q^6}. \tag{10}$$

6. Summary and Discussions

A new technique which is capable of systematically inducing rotation on a levitated metallic drop in vacuum was used for the study of dynamics of rotating charged drops, and an alternate technique of measuring the surface tension was verified. Although the drops carried surface charges, the experimental results showed close agreement with the Brown & Scriven's theory. This experiment showed that the surface charge on the drops (although aluminum had 24%, and tin had as much as 41% of their respective Rayleigh charge limits) did not cause any deviation from the prediction. This result is consistent with the previous results obtained from rotating charged water drops[4]. Good agreement with the prediction was possible only when the condition of solid-body rotation was abided. Under the influence of high level torque, the bifurcation of drop shape did not occur at the predicted point. Instead, the axi-symmetric branch overshot the bifurcation point before it transformed into the two-lobed branch. An anomalous behavior was observed in a rotating tin drop which showed strong deviation from the prediction. We speculated that this anomaly was caused by isotope separation under the influence of centrifugal force.

The surface tension measurement technique based on sample rotation was tested using a molten tin and an aluminum drops. The effective oscillation frequency obtained from the rotation experiment near the bifurcation point agreed with the actual oscillation frequency within ±2%. This is an encouraging result in view of the fact that we now have a non-contact method of measuring surface tension of viscous liquids to which the drop oscillation method cannot be applied. Also, this technique will be well utilized in the future development of a non-contact viscosity measurement technique for high viscosity liquids. The area where these new techniques may be valuable might be the group of bulk-glass-forming alloys which show viscosity increasing more than 12 orders of magnitude as they approach glass-formation temperatures. Work along this line is under way.

Acknowledgments:

The authors would like to acknowledge Dr. Paul-Francois Paradis for his help in taking some data, Mr. D. Barber for hardware fabrication, and Mr. Eugene Rhim for proof reading of this manuscript. This work was carried out at the Jet Propulsion Laboratory, California Institute of Technology, under contract with the National Aeronautics and Space Administration.

References:

[1 Lord Rayleigh, Phil. Mag. 28, 161, 1914.

[2] S. Chandrasekhar, "The Stability of a Rotating Liquid Drop," Proc. Roy. Soc. London, A 286, 1, 1965.

[3] R. A. Brown and L. E. Scriven, "The Shape and Stability of Rotating Liquid Drops," Proc. R. Soc. Lond. A 371, 331, 1980.

[4] W-K. Rhim, S.K. Chung, and D.D. Elleman, "Experiments on Rotating Charged Liquid Drops," Proc. 3rd International Colloquium on Drops and Bubbles (ed. T. G. Wang), AIP Conf. Proc. 197: 91, 1988 .

[5] A. Biswas, E. W. Leung, and E. H. Trinh: "Rotation of ultrasonically levitated glycerol drops", J. Acoust. Soc. Am. 90, 1502-1507, 1991.

[6] T. G. Wang, E. H. Trinh, A. P. Croonquist, and D. D. Elleman, "Shapes of Rotating Free Drops: Spacelab Experimental Results," Phys. Rev. Let. 56, 452, 1986.

[7] [11] T. G. Wang, A. V. Anilkumar, C. P. Lee and K. C. Lin: "Bifurcation of rotating liquid drops: results from USML-1 experiments in Space", J. Fluid Mech. 276, 389-403, 1994.

[8] W. K. Rhim, K. Ohsaka, P-F. Paradis and R. E. Spjut, "A non-contact technique of measuring surface tension and viscosity of molten materials using high temperature electrostatic levitation", Rev. Sci. Instrum. (in press)

[9] W. K. Rhim, S. K. Chung, D. Barber, K. F. Man, G. Gutt, A. Rulison, and R. E. Spjut, "An Electrostatic Levitator for High Temperature Containerless Materials Processing in 1-g," Rev. Sci. Instrum. 64: 2961, 1993.

[10] S. A. Nasar and I. Boldea, Electric Machines (Steady tate Operation), Hemisphere Publishing Corporation, 1990.

[11] P. L. Alger, Nature of Induction Machine, Gordon and Breach Science Publishers, 1965.

[12] D. D. Elleman, T. G. Wang, and M. Barmatz, "Acoustic Containerless Experiment System: A Non-Contact Surface Tension Measurement," NASA Tech. Memo. 4069, Vol. 2, 557, 1988.

[13] Lord Rayleigh, Phil. Mag. "On the Equilibrium of Liquid Conducting Masses Charged with Electricity," 14, 184, 1882.

[14] Q. Feng and K. V. Beard: Proc. Roy. Soc. Lond. A. 430, 133, 1990

Table I: Parameters relevant to samples used to obtain the data shown in Fig. 3.

Samples	Aluminum	Tin
Weight (mg)	26.5	27.1
Melting point T_m (°C)	660.5	232
Sample temperature (°C)	705	320
Density at T_m (g/cm^3)	2.38	6.98
Surf. Tension at T_m (mN/m)	914	560
Viscosity at T_m (mP·sec)	2	1.81
Net Electric Charge (nCoul.)	0.445	0.3451
Rayleigh Limit (nCoul.)	1.843	0.851
$Q/Q_{Rayleigh}$ (%)	24.16	41.2

Figure Captions:

Fig. 1. Top and side views of the electrode assembly used for the present experiment.

Fig. 2. Torque versus normalized sample rotation frequency measured using an aluminum sphere at three different applied currents.

Fig. 3. Normalized drop size versus normalized drop rotation frequency of both molten tin and aluminum drops are compared with the theoretical curves obtained by Brown and Scriven. Those dat points marked by arrows correspond to the drop shapes shown in Fig. 4.

Fig. 4. Side views of a rotating aluminum drop each of which corresponding to a data point in Fig. 3 marked by an arrow.

Fig. 5. Anomalous behavior of a rotating tin drop when it was kept for two hours at a two-lobed drop shape.

Fig. 6. The shape of the anomalous tin (of Fig. 5) when it finally came to rest.

Fig. 7. Shape evolutions of rotating aluminum and tin drops were plotted in terms of R_{max}/R_{min} versus $\omega_{rot}/\omega_{osc}$.

Fig. 8. The result after the normalization of data points shown in Fig. 7.

Fig. 9. The effective oscillation frequencies obtained from the deforations of a tin drop rotated at different frequencies are compared with the directly measured oscillation frequency of the same drop.

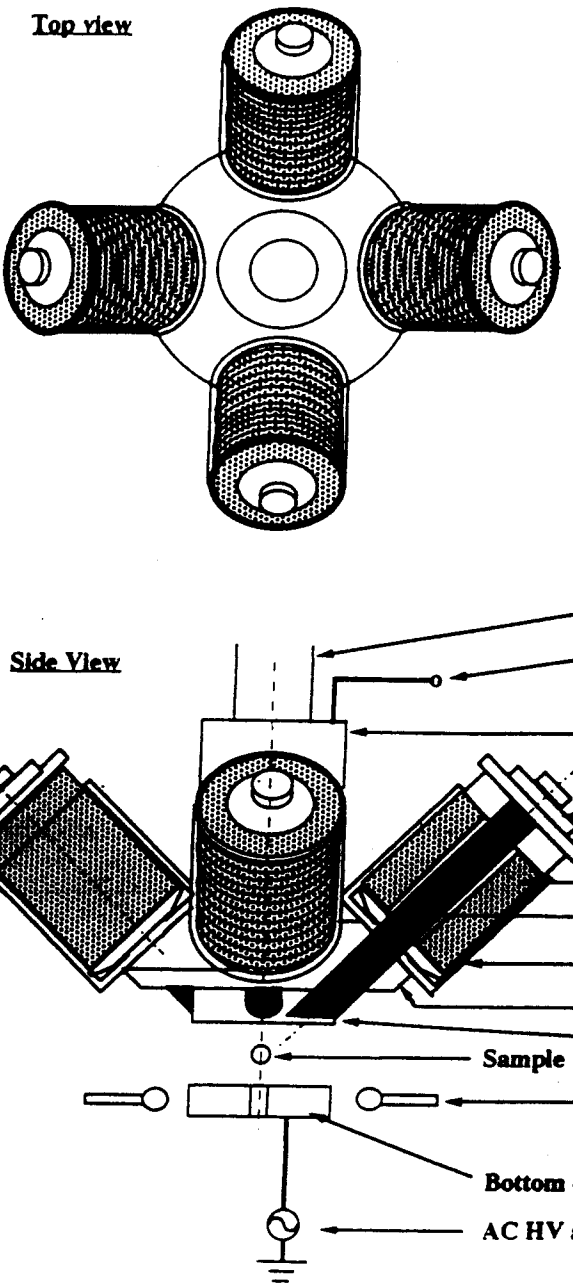
Top view
Side View
Macor rod
To HV amplifier
Copper heat sink
Glass spool
Coils (4)
Soft iron core
Glass insulator
Macor coil holder
Top electrode
Sample
Side electrodes(4)
Bottom electrode
AC HV amplifier

Fig. 1

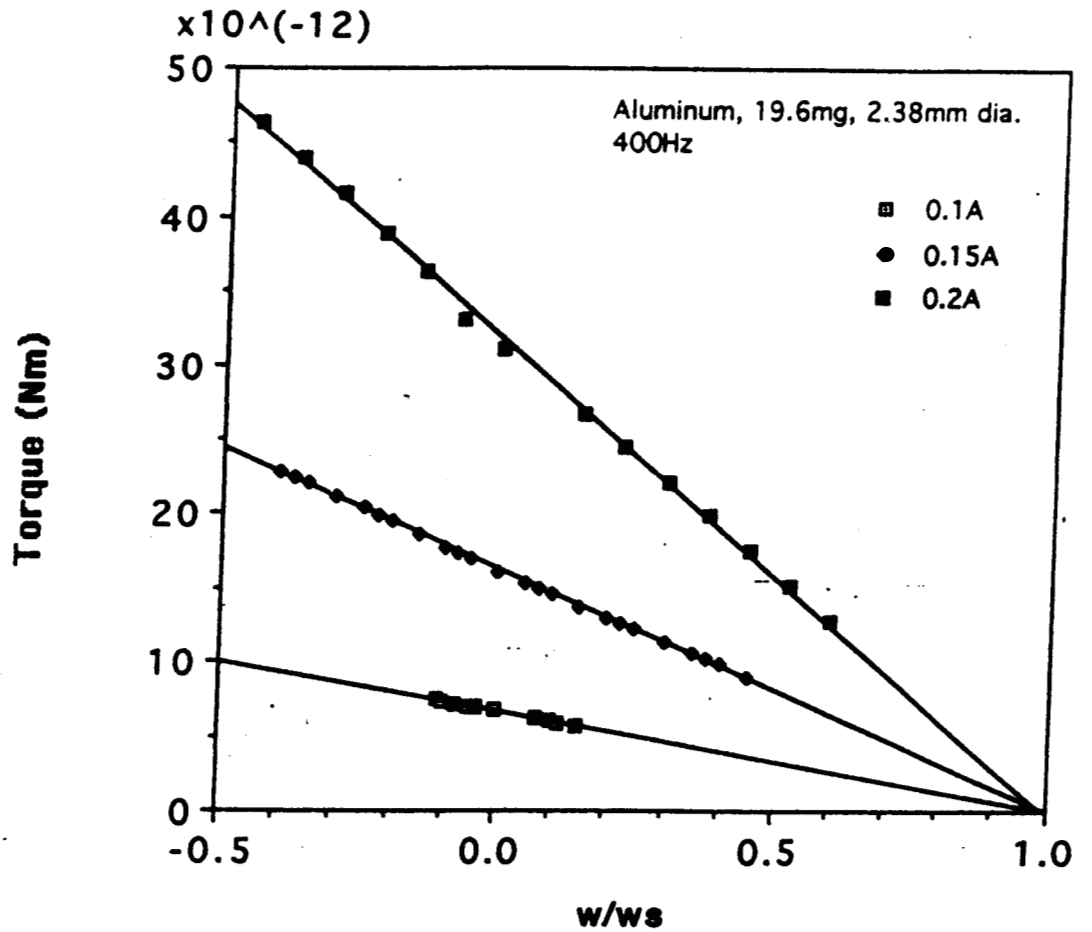
x10^(-12)
50
40
30
20
10
0
Torque (Nm)
Aluminum, 19.6mg, 2.38mm dia.
400Hz
0.1A
0.15A
0.2A
-0.5
0.0
0.5
1.0
w/ws

Fig 3

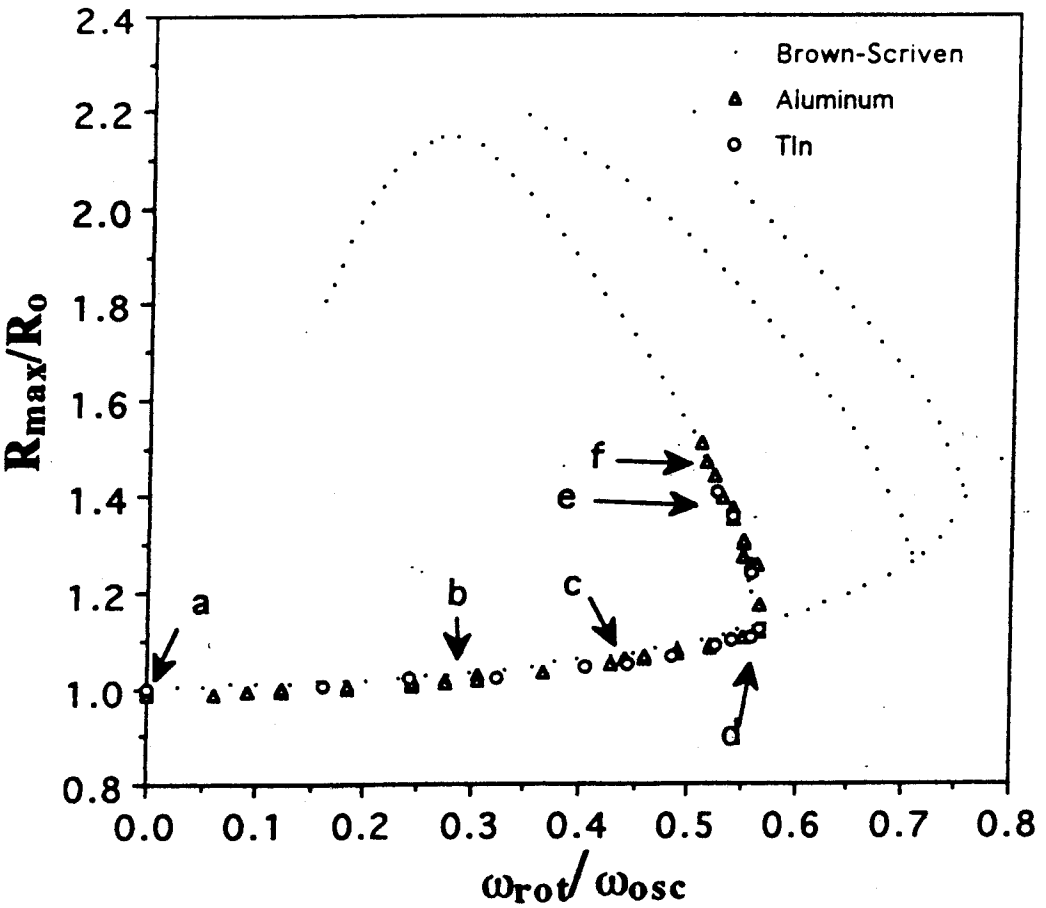
Brown-Scriven
Aluminum
Tln
R_{max}/R_o
$\omega_{rot}/\omega_{osc}$
2.4
2.2
2.0
1.8
1.6
1.4
1.2
1.0
0.8
0.0
0.1
0.2
0.3
0.4
0.5
0.6
0.7
0.8
a
b
c
d
e
f

Fig 3

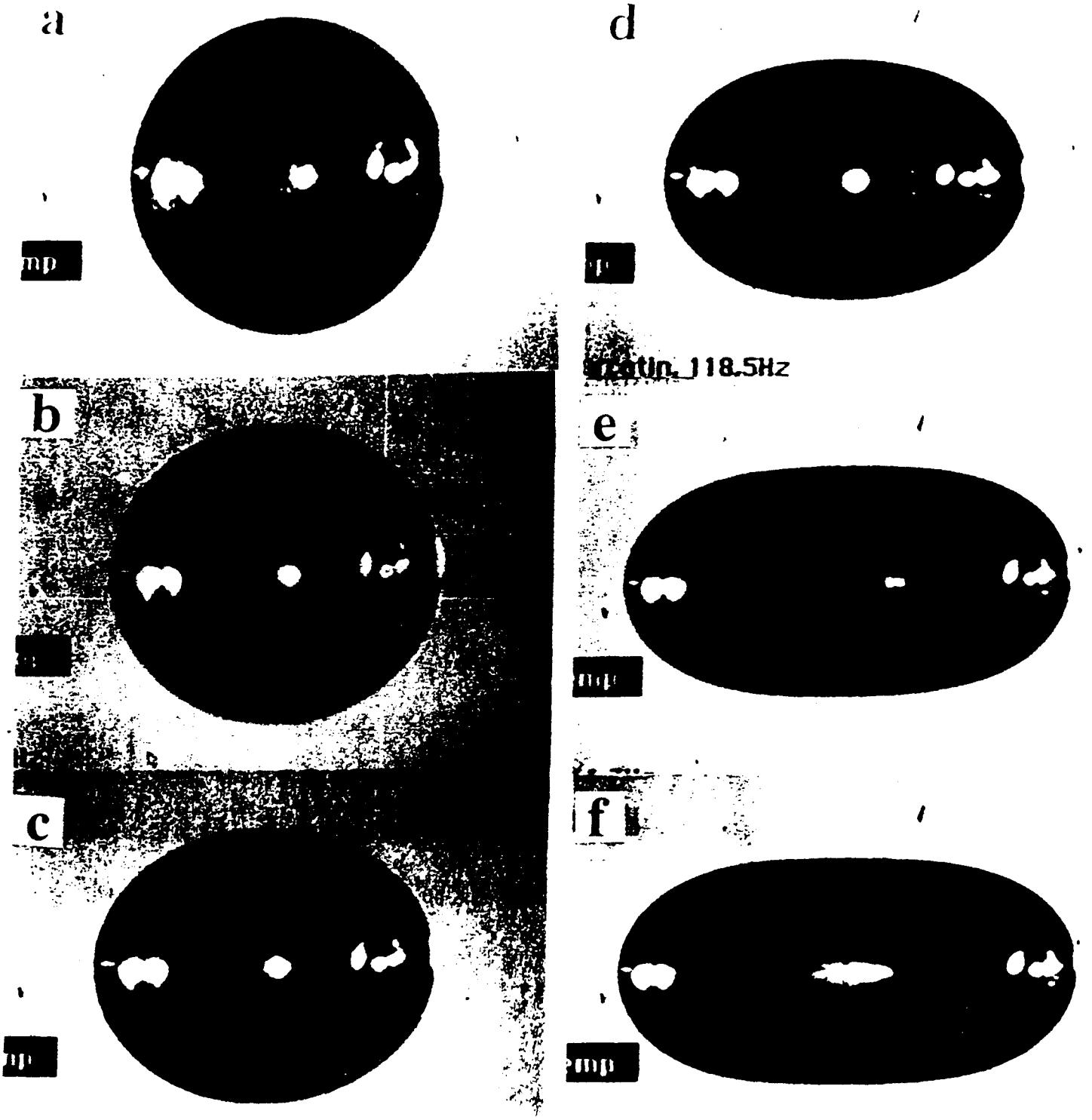
a
d
b
e
c
f

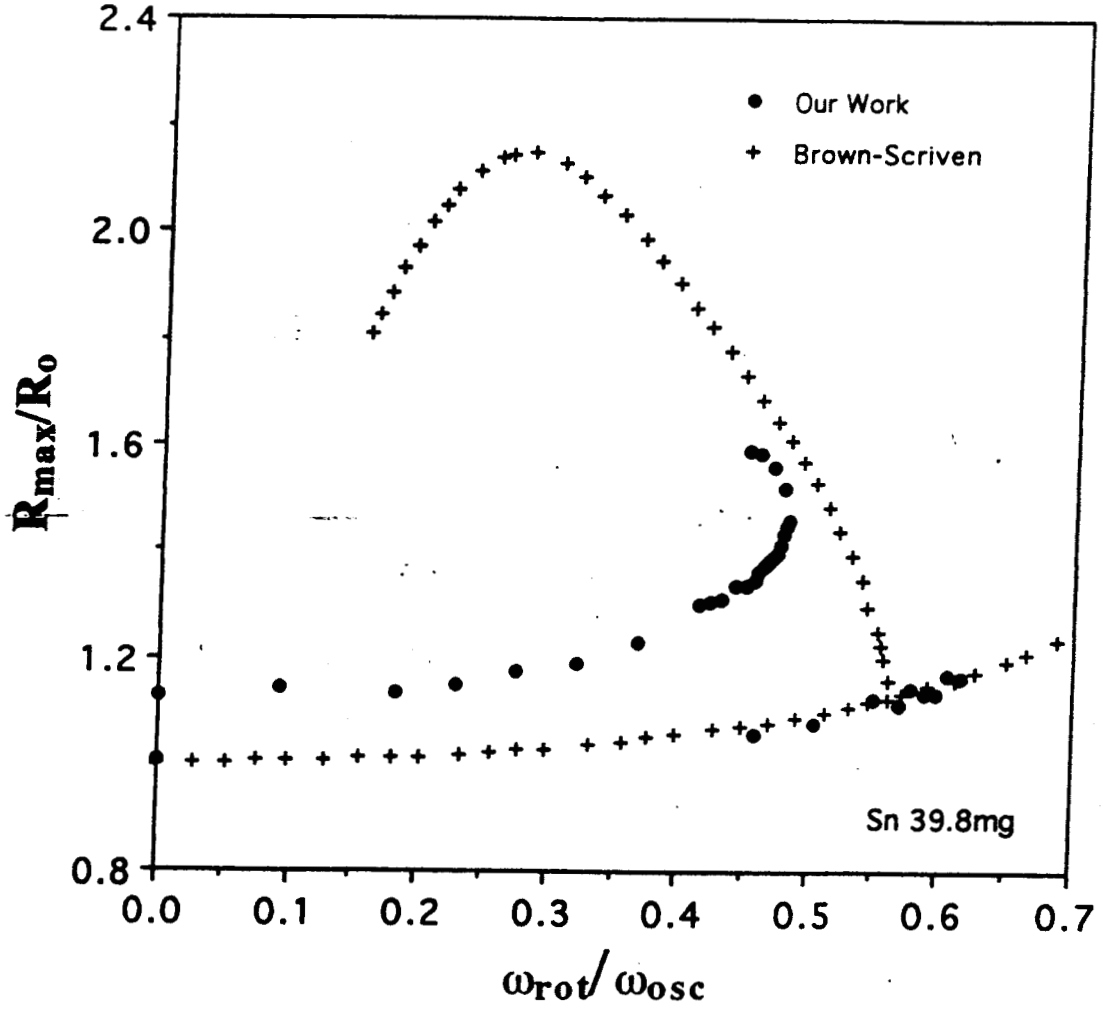
Our Work
Brown-Scriven
Sn 39.8mg
R_{max}/R_o
$\omega_{rot}/\omega_{osc}$
2.4
2.0
1.6
1.2
0.8
0.0
0.1
0.2
0.3
0.4
0.5
0.6
0.7

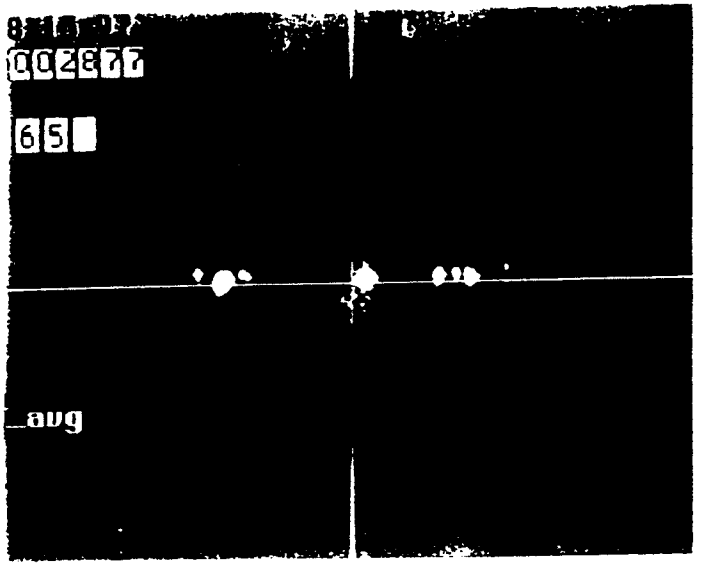
65
_avg

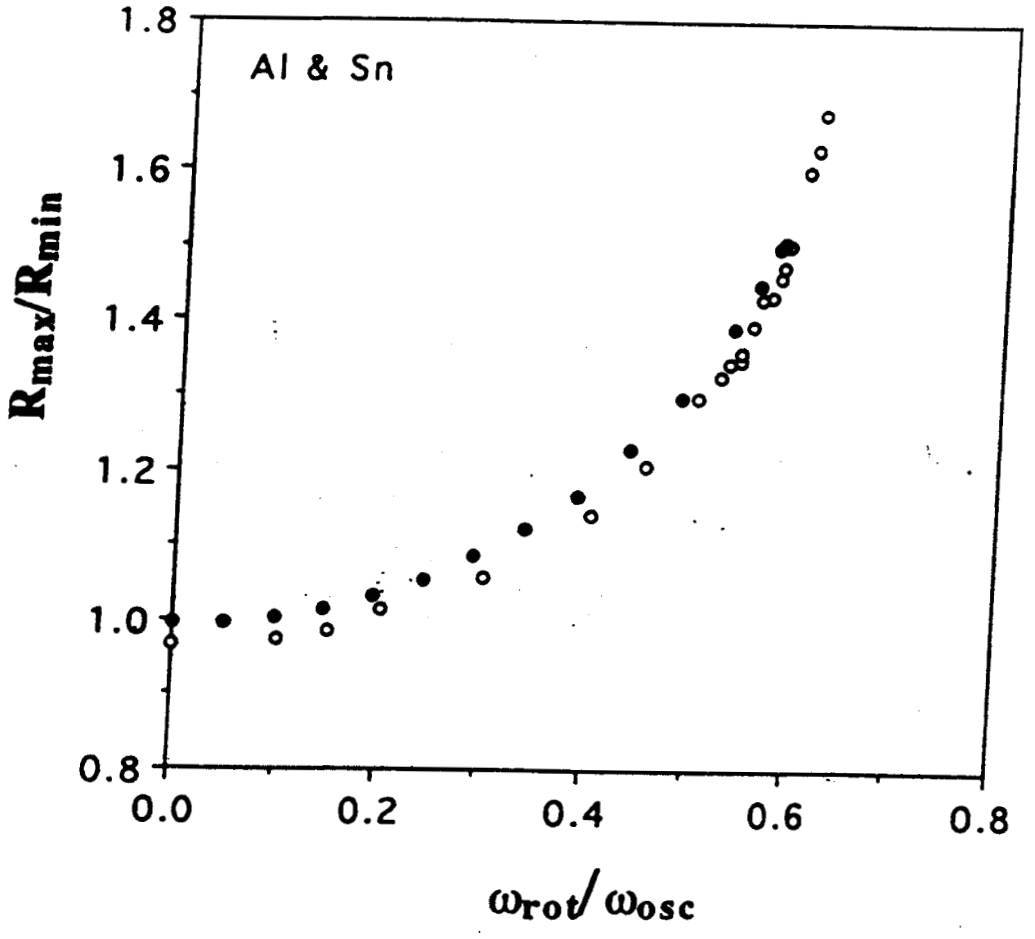
Al & Sn
1.8
1.6
1.4
1.2
1.0
0.8
0.0
0.2
0.4
0.6
0.8
R_{max}/R_{min}
$\omega_{rot}/\omega_{osc}$

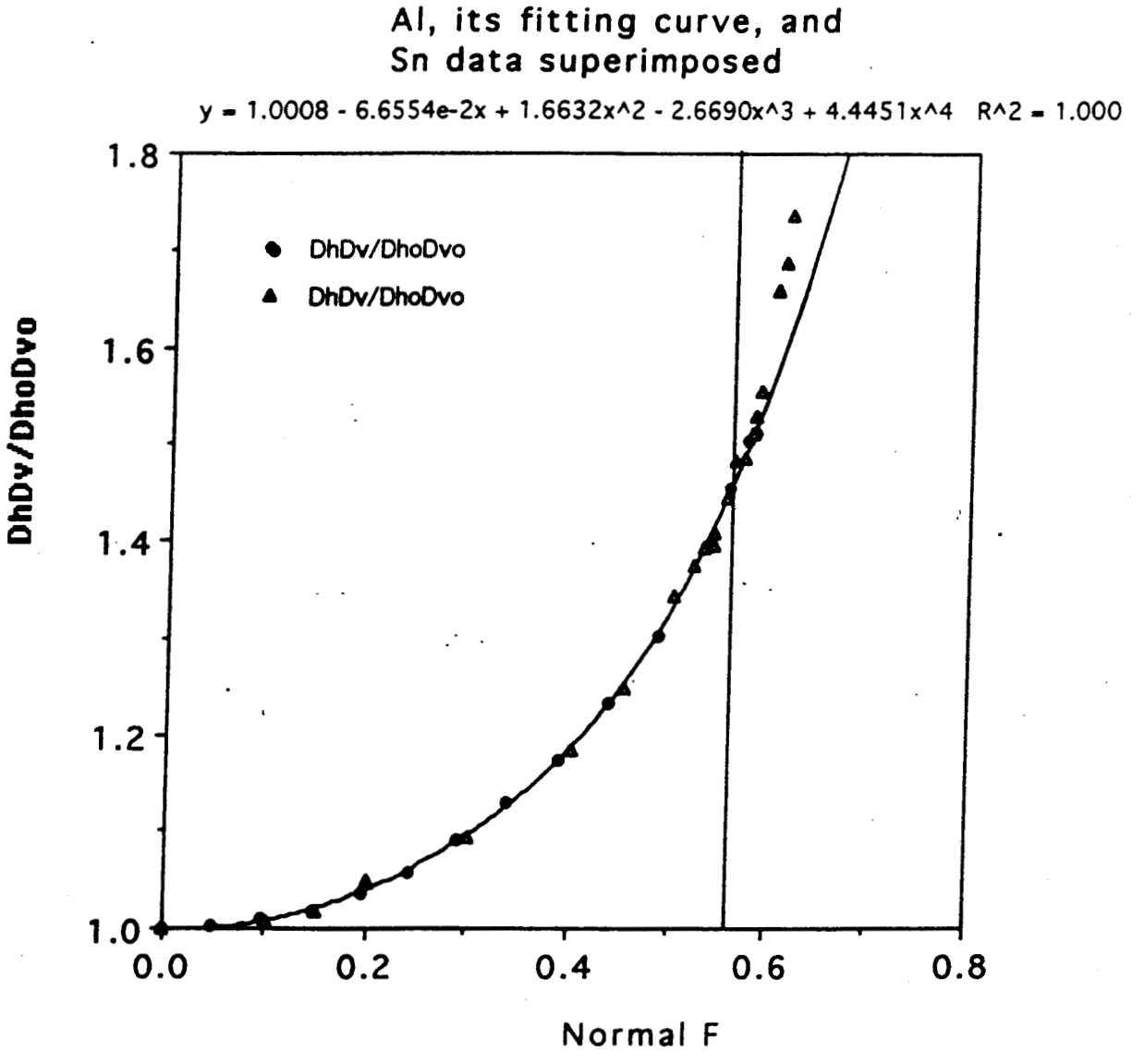
Al, its fitting curve, and
Sn data superimposed
y = 1.0008 - 6.6554e-2x + 1.6632x^2 - 2.6690x^3 + 4.4451x^4 R^2 = 1.000
DhDv/DhoDvo
DhDv/DhoDvo
DhDv/DhoDvo
1.8
1.6
1.4
1.2
1.0
0.0
0.2
0.4
0.6
0.8
Normal F

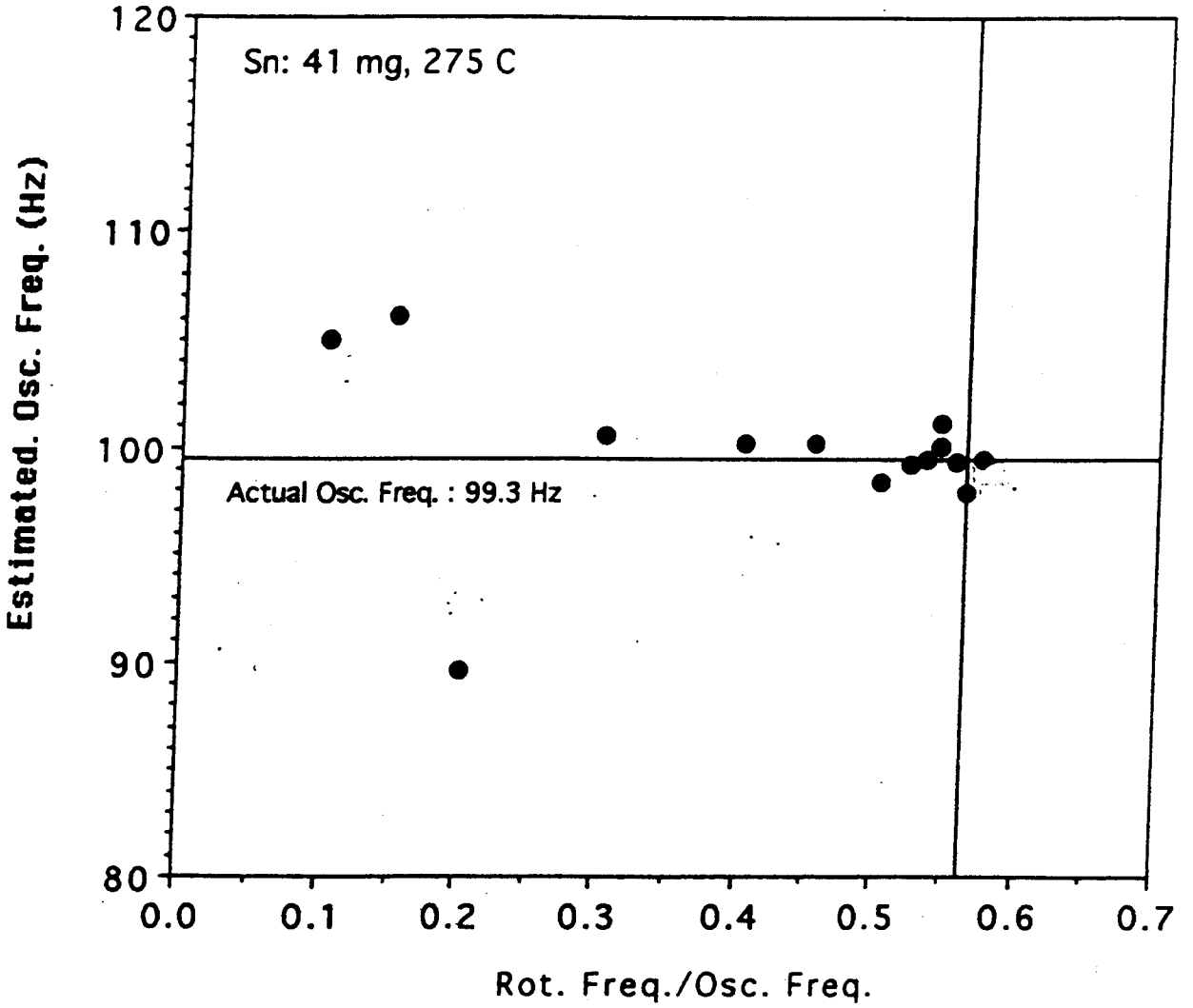
Sn: 41 mg, 275 C
Actual Osc. Freq. : 99.3 Hz
Estimated. Osc. Freq. (Hz)
120
110
100
90
80
0.0
0.1
0.2
0.3
0.4
0.5
0.6
0.7
Rot. Freq./Osc. Freq.